Journal of Tropical Resources and Sustainable Science
Website : http://journal.umk.edu.my/index.php/jtrss/
eISSN : 2462-2389
Vol: 14, Issue 2, 2026, 325-334
DOI: https://doi.org/10.47253/jtrss.v14i2.1662

RESEARCH ARTICLE

Structural geology analysis using Electrical Resistivity Imaging (ERI) In Felda Chiku 5, Paloh, Gua Musang, Kelantan.

Mahendra Abiyoga Hidayat, Mohd Syakir Sulaiman*

Geoscience Department, Faculty of Earth Science, University of Malaysia Kelantan, 17600 Jeli, Malaysia

ARTICLE HISTORY
Received : 27 July 2025
Accepted : 8 December 2025
Online : 30 June 2026

KEYWORDS
Electrical Resistivity Imaging (ERI), fault,
Structural Geology

☒ * **CORRESPONDING AUTHOR**
Geol. Dr. Mohd Syakir Sulaiman,
Geoscience Department,
Faculty of Earth Science,
University of Malaysia Kelantan,
17600 Jeli, Malaysia.
Email: syakir.s@umk.edu.my

ABSTRACT

The research area was located in the Gua Musang district, and the method employed was Electrical Resistivity Imaging (ERI). Geophysics is the study of physical processes that take place on a variety of scales, from microscopic to planetary and interplanetary. To support the data for interpretations of the underlying structure, geophysical methods were developed. In addition to being very affordable, geophysical technologies may instantly deliver data with excellent precision. Two-dimensional resistivity imaging techniques were employed in this study to look at the geological structures. This approach is reliable for giving precise information on the subsurface, including bedrock depth, overburden material characteristics, and features close to the surface, such as bedding, faults, folds, fractures, and contact zones. Using 2-D resistivity imaging, data is promptly and accurately provided, making it simpler to analyse. Three survey lines were employed to assess the subsurface structural geology of the Felda Chiku 5 area. The first and second survey lines employed a gradient electrode configuration, but the third line used a pole-dipole array with electrode spacing of 5 meters for a 200-meter line spread each. The ABEM Terrameter LS was used to measure resistivity. Following data collection, the activity proceeds to data processing and inversion using the RES2DINV application by projecting resistivity measurements onto a 2D profile and evaluating the resulting data. The pseudosection model displayed variable resistivity values at a depth of inquiry of around 36 meters to 57 meters and a range of 1Ωm to >2500Ωm. According to the model, the research area's structural investigation revealed fault lines in the subsurface region. Subsurface movement was indicated by the fault line. In order to provide the amount of knowledge on underlying geological structures for geoengineering study for site inquiry, this study recommends that additional geophysical investigation (seismic survey) be conducted.

1. INTRODUCTION

Structural geology investigates rock deformation caused by tectonic forces, gravitational impacts, and internal Earth processes. It studies the geometry, distribution, and formation mechanisms of geological features, including folds, faults, joints, and foliations (Alamu & Dada, 2025).

Geophysical methods have been increasingly popular in recent years, particularly in engineering and environmental investigations. Geophysics is a branch of physics that is used to study the Earth. Geophysical methods are well-known for being cost-effective, quick, and easy to handle. Resistivity, density, magnetic, seismic, and other methods are the most commonly used (Hazreek et al., 2018). Because resistivity methods are effective at mapping subsurface data, engineers have used them in soil investigation (SI) work in the past. The electrical resistivity approach has made significant strides in recent years in terms of survey coverage, field measurement, processing methods, and identification of geological features in the subsurface profile (Abidin et al., 2017). ERI was designed to map and assess subsurface materials' resistivity (Thiagarajan et al., 2018). It also refers to a survey that is used to offer an image of the electrical qualities of the subsurface by conducting an electrical current through a variety of routes and measuring the voltage that results (Hutchison & Denis, 2009). In the resistivity method, there are five types of electrode configurations, such as Wenner, Schlumberger, Dipole-dipole, Pole-dipole, and Pole-pole (Muzamil et al., 2016). The purpose of ERI was to measure and map the resistivity of subsurface materials (Thiagarajan et al., 2018). It also refers to a survey that is used to offer an image of the electrical qualities of the subsurface by conducting an electrical current through a variety of routes and measuring the voltage that results (Hutchison & Denis, 2009).

Resistivity also describes a survey that uses a number of methods to conduct an electrical current and

measure the voltage that occurs in order to provide an image of the electrical structure of the subsurface. A deeper understanding of the underlying geological conditions that may have prevented any serious effects, like the subsurface fracture that destroyed the main road, was made possible by the extensive geological and geophysical research utilized to determine the tectonic geological features (faults), and subsurface movement was indicated by the fault line (Sulaiman & Abiyoga, 2023).

By utilizing electrical resistivity and chargeability to identify the subsurface structures, depths, and lateral spread of the lithological strata, the ERI and IP, together referred to as the geoelectrical techniques deployed, can quickly evaluate the target's zones below the surface. The techniques have been applied to prospect for economically viable and naturally occurring resources, characterize subterranean geological structures in a variety of ways, and offer long-term solutions to environmental problems and geohazards because of the successes. Numerous researchers have created a range of electrode array configurations to generate fruitful data analysis outcomes. The same procedures used for electrical resistivity are also used for induced polarization. The IP procedure differs from the ERI in that it calculates the earth material's apparent chargeability, which is measured in milliseconds or millivolts per volt. Certain subsurface components, or metallic grains (a metal sulfide), which function as ions inside rock bodies, may become electrically polarized, which stores electrical charges when an electrical current is introduced into the Earth (Zaid et al., 2023).

Peninsular Malaysia is divided into four structural zones: northwest, west, central, and east. Throughout the Palaeozoic, the Northwest structural domain contains NE striking structures, a contact aureole, and continuous deposition (Kasim et al., 2020). The structural trend in the Western domain is NNW and N, with major tectonic movement westward, while the structural grain in the Central domain ranges between North and NNW. The Bentong-Raub line to the west and the Labir Fault zone to the east define the Central extensional graben. The regional structural trend in the Eastern domain is NW to NNW. The region has granitic, sedimentary/metasedimentary, extrusive (volcanic), and unconsolidated deposits. Western and eastern state borders have granitic rocks. Main Range Granite reaches north to Thailand from the BRSZ's boundary. The Lebir Fault Zones are one of Peninsular Malaysia's primary lineaments.

In the Western Belt, most of the rocks are clastic and carbonate sediments, with a few volcanic rocks here and there. The Main Range is made up of granitic rocks from the Triassic, and the belt is made up of rocks from the Palaeozoic, a margin sequence that was linked to the northwest Australian portion of Gondwana until the early Permian (Metcalfe, 2002). Palaeozoic sediments are found in most locations, with Mesozoic rocks scattered throughout Kedah and northern Perak. The Kinta Valley has carbonate limestones ranging from the Silurian to the Permian epochs, but other sites have metasediments and lower Palaeozoic limestones.

The major rocks of the Central Belt, which is an extensional graben limited to the west by the Bentong-Raub suture zone and to the east by the Lebir Fault Zone, are deposits of Palaeozoic and Triassic rocks, with some Jurassic and Cretaceous rocks in small amounts. Marine carbonate sediments, shales, volcanic-clastic, and andesites are among the deposits found here. North of the band, shallow marine sediments from the Permian to Lower Triassic. There are marine Permian strata from the Gua Musang Formation, Aring Formation, and Kepis Beds in the Paleozoic and Mesozoic periods, as well as carbonaceous rocks from the Semantan Formation and the red siliciclastic Paloh Formation in the latter period (Kasim et al., 2023).

The Eastern Belt contains two primary depocenters: Permian clastic marine sediments south of West-northwest-east-southeast (WNW-ESE) striking Lepar fault and Carboniferous metasediments north. Palaeozoic sediments unconformably overlie Jurassic - Cretaceous continental deposits. Carboniferous sediments (Kuantan Group, Kamning and Seri Jaya beds) and Permian conglomerates dominate (Linggui and Dohol formations) (Kasim et al., 2020).

During the period of the Carboniferous, East Malaya was attached to the Indochina plate, and Sibumasu was attached to the Gondwana; it became a part of the Cimmerian plate (Jasin, 2013). But from the Devonian to the Permian, an ocean called the Palaeo-Tethys kept the Sibumasu and East Malaya blocks apart.

Middle Permian-Middle Triassic sediments from the Gua Musang Formation are comprised of crystalline limestone interspersed with thin layers of shale, tuff, and chert nodules (Mohamed et al., 2016). The Gua Musang Formation stratigraphic model, burial history, and geothermal model were developed by examining three outcrops of the formation. Sandstone and conglomerate make up the first outcrop, followed by limestone, shale, and siltstone in the next two (Folk & Bissell, 2022).

Gua Musang, Kelantan, is part of Peninsular Malaysia's Central Belt, which spans from Kelantan to Johor. In the western half of the Central Belt, you can find the Upper Palaeozoic Gua Musang and Aring Formations in south Kelantan and the Taku Schist in east Kelantan. The Gua Musang Formation is made up of crystalline limestone that is thought to be 650 meters thick (Sulaiman, 2021). Thin layers of shale, tuff, chert nodules, and subordinate sandstone and

volcanics are mixed in with the limestone. Calcitic limestone is hard, doesn't have pores, breaks easily, and has sharp edges with a light gray color. Limestone that has been recrystallized often has a gray to black color and contains minimal levels of carbonaceous, argillaceous, and pyroclastic impurities (Mah, 2018). Taku Schist and the Gua Musang Formation are geologically present in Negeri Kelantan. Granite, diorite, andesite, ignimbrite, and dolerite are igneous rocks in Negeri Kelantan. (Yao et al., 2017).

Granite intrusion and diorite pop-up towards NE-SW characterize the northern portion of this major fold. Dextral faults are the most common in the Gua Musang Formation. The Gua Musang Formation created compact and firmly folded areas bordering igneous granite intrusions and near the main fault. To follow this diorite intrusion, the major fold of the Gua Musang Formation has been named. The major compression caused the Gua Musang Formation to fold and fault (Yao et al., 2017).

Paloh's geological structure is composed of both sedimentary and volcanic rocks. Volcanic breccia, ignimbrite, tuff, and volcanic sandstone are part of the pyroclastic rocks. However, conglomerate, carbonaceous mudstone, sandstone, and mudstone are components of sedimentary rocks (Sulaiman & Abiyoga, 2023).

The primary faults in the Gua Musang Formation are the sinistral fault, which has a strike of N330-340° E and dips 60-80° to the ENE-WSW, and the

dextral fault, which has a strike of N30-45° E and dips 60-70° to SE. The Gua Musang Formation created a compact and highly folded region in the vicinity of the major fault and in the zone bounded by igneous granite intrusion. The major fold of the Gua Musang Formation must be termed to follow this intrusion of diorite porphyry. The Gua Musang Formation's folding and faulting were mostly caused by compression that occurred between the WNW-ESE and ENE-WSW (Meetings of the Society, 2017).

This study is important to provide an interpretation of 2-D resistivity methods, and can also investigate the subsurface condition, such as geological features, rock structure, and potential underground water resources. Research can be significant and is important to the district council, engineers, public, and management. A new finding of geological features present in the study area can also help people to have a better understanding of the geological condition that occurs in that area.

2. MATERIALS AND METHODS

2.1. Study area

This research was carried out at Felda Chiku 05, Paloh, Gua Musang, Kelantan, with the coordinates of 4°58'17.5"N, 102°12'0.6"E. Felda Chiku 05, Paloh, is in the Southeast of the Gua Musang district. This study area is surrounded by Masjid Al-Ghufran Felda Chiku 05 & 06 and Balai Raya Felda Chiku 5. The highest elevation that can be found at Felda Chiku 05 is 200 m, and the lowest will be 80m above sea level. The main river at Felda Chiku 05 area is called Sungai Chiku and Sungai Gasing (Figure 1-2).

The study area was composed of sedimentary rock, which, because of the metamorphism process, has begun to transform into metasedimentary rock. In the period known as the Early to middle Triassic, sedimentary rock limestone was metamorphosed into marble, which is mostly found in streams and rivers. However, in the Late Triassic, meta-sedimentary rock in the form of meta-mudstone and meta-quartz was formed. According to the age of the rocks, the deposition of marble happened first, followed by meta mudstone and meta quartz wacke. The major fault that is in the middle of my study area is the boundary between the formation of meta quartz wacke and meta mudstone rock.

Paloh is an agricultural area that is developed by the South Kelantan Development Authority (KESEDAR). It is composed of three distinct plans, which are referred to as Paloh 1, Paloh 2, and Paloh 3. The research site Felda Chiku 05 is located next to Paloh 2, which has an oil palm plantation of 1113.80 hectares and a rubber plantation covering 480.86 hectares. The remainder consists of protected areas of forest. (Hussin & Abdullah, 2012). Palm oil plantations and rubber estates make up most of the study area, with palm oil plantations accounting for around 60% of the total area and rubber plantations, settlements, and forest areas accounting for the remaining 40%. Rural, industrial, leisure, transportation, commercial use, and land for vegetation are some of the land use types. Much of the area is covered with forests, natural forests, or rubber plantations. Other than plantation land use, such as a residence area, shops, a police station, and a mosque.

Gua Musang, Kelantan, is part of Peninsular Malaysia's Central Belt, which spans from Kelantan to Johor. In the western half of the Central Belt, the Upper Palaeozoic Gua Musang and Aring Formations will be found in south Kelantan and the Taku Schist in east Kelantan. The Gua Musang Formation is made up of crystalline limestone that is thought to be 650 meters thick (Sulaiman, 2021).

In the Paloh region, four distinct lithological units may be found. Tuff, mudstone, and andesite units comprise the metasediment unit of the Middle Permian period. The metasediment unit is the oldest rock unit. A tuff unit from the Early Triassic period has been deposited above the

unconformity. The Middle Triassic mudstone unit lies on top of the unit's conformity. Mudstone and siltstone make up the mudstone unit. Unconformity on the mudstone unit is overlain by the youngest Late Triassic andesite unit (Xin, 2018). Andesite lava and tuff make up most of the structure. Hit-slip faults strike the research region from the NNW-SSE and NNE-SSW directions. (Mah, 2018).

Figure 1: Satellite image of a) Malaysia map, b) Kelantan map, c) Gua Musang, d) Paloh, and e) Felda Chiku 05

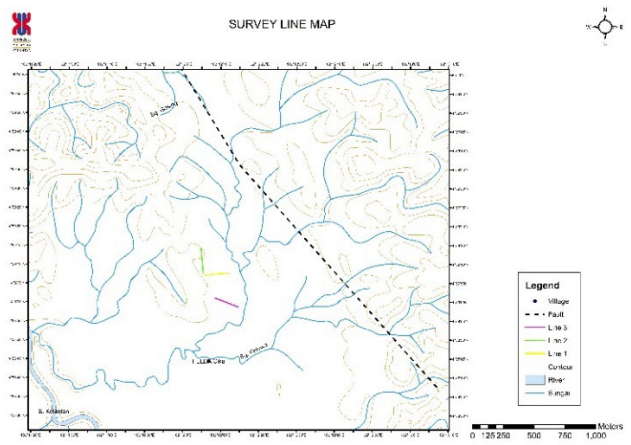

Figure 2: Survey line location map

2.2. Methodology

This survey was carried out to identify the subsurface faulting at Felda Chiku 05, Paloh area. The geophysical method used was Electrical Resistivity Imaging (ERI) with a suitable electrode array configuration. There are several types of electrode arrangement, such as Wenner, Schlumberger, Pole-pole, Dipole-pole, Dipole-dipole, and Gradient. The electrode arrangement that had been used was determined based on the objective of the study.

Different electrode arrangement covers different depths. Wenner covers less depth compared to Schlumberger, while Pole-dipole results in the greatest depth. The Wenner array provides information about the structure. Reading from 3 survey lines was collected using a Gradient and a Pole-dipole array with electrode spacing of 5m for 200m lines. The potential energy between two adjacent current electrodes is read to obtain a measurement using the Gradient Array. The transmitter dipoles A&B are used to measure the lateral variations in the Gradient Array's potential field. The process of profiling is sometimes referred to as recording lateral changes (Sean, 2019). A gradient array is something similar to a Schlumberger array, but a Schlumberger array only records the receiver from the centre dipole, whereas a gradient array measures all adjacent dipoles. A pole is a solitary communicating cathode, and a dipole is a pair of oppositely charged terminals that are so close to one another that the electric field looks like a single electrode instead of 2 different ones. Pole-dipole provides a clearer picture of the cross-section of the Earth (Hasan, 2017).

The ABEM resistivity system measures the Earth's subsurface resistance. ABEM resistivity systems include Terameter LS, multifunctional cable, 40 jumper cables, 41 stainless-steel electrodes, a 12-volt battery, and a remote cable. Different electrode arrangement covers different depths. Wenner covers less depth compared to Schlumberger, while Pole-dipole results in the greatest depth. The Wenner array provides information about the structure trace. Reading from 3 survey lines was collected using a Gradient and a Pole-dipole array with electrode spacing of 5m for 200m lines. The result of apparent resistivity shows in Terrameter LS Toolbox value that inverted using software to determine the true resistivity. Resistivity data were then analysed using the Res2Dinv software. The RES2DINV program is used to process raw field data and produce the 2D resistivity inversion pseudo-section model, which shows the resistivity values of the subsurface region. The inversion's results have an RMS inaccuracy of less than 20%. Following that, the result is contrasted with the standard materials' resistivity value established by previous studies, which is shown in Table 1. Figure 3 provides a very broad overview of the potential chargeability of materials. Large amounts of mixed materials are used in field measurements, which is one reason why in-situ chargeabilities often look lower than laboratory values. These examples demonstrate that a broad range of variability may be anticipated, suggesting that it is challenging to precisely identify the kind of rock or material in the ground using values of inherent chargeability in models produced by inversion of IP data.

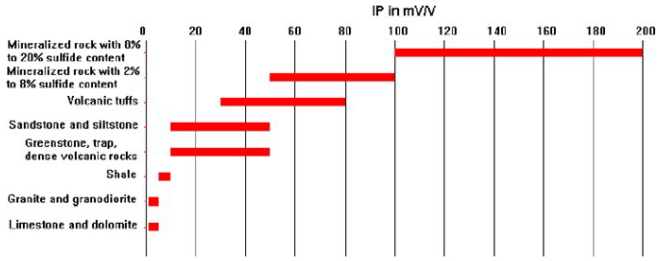

Figure 3: IP values for some rocks and minerals in mV/V (Amadasun et al., 2015)

RES2DINV software was known as a 2D inversion software. The software worked very easily, as it imported data for inversion and visualization. It supported all electrode configurations and cross-borehole surveys ("Geotomo Res2DInv," 2020). The results are then interpreted using the comparison. Terrameter LS Toolbox was a software by ABEM Instruments, which may be used to calculate IP as well as pre-process raw DCR data that has been obtained by Terrameter LS. It provided the user's ability to access raw field data acquired with Terrameter LS, display it in a variety of different ways, and export it into a preferred format.

Table 1: Resistivity Values of Common Rocks, Minerals, and Chemicals (Loke, 2001)

MATERIAL	RESISTIVITY (Ωm)
Igneous and Metamorphic Rocks	
Granite	5×10^3 - 10^6
Slate	10^3 - 10^6
Basalt	6×10^2 - 4×10^7
Marble	10^2 – 2.5×10^8
Quartzite	10^2 - 2×10^8
Sedimentary Rocks	
Sandstone	8 - 4×10^3
Shale	20 - 2×10^3
Limestone	50×10^2 - 4×10^2
Soils and waters	
Clay	1-100
Alluvium	10 - 800
Groundwater (fresh)	10 - 100
Sea water	0.2
Chemical	
Iron	9.074×10^8
0.01 M Potassium Chloride	0.078
0.01 M Sodium Chloride	0.843
0.01 M Acetic acid	6.13
Xylene	$6.998\ 10^{16}$

A model section was used to get the apparent resistivity value, and this model section is referred to as the pseudo-section. The apparent resistivity depends on the shape of the electrode hence, it cannot reflect the actual subsurface state. Understanding the subsurface through apparent resistivity reading requires inversion. The resistivity scale operates in the opposite direction in the model portion. The resistivity value, according to the industry norm for earth materials, provides a good approximation of the layer's depth.

If the rock's pore fluid is being displaced, the rock's resistivity value will be high. This is because during lithification, the minerals get compacted and block the passage of electric current. A similar phenomenon occurs when the salinity of the pore fluid is low, leading to an increase in the resistivity value. The quantity of salt that can be dissolved in each fluid is directly proportional to its saltiness. The activity of ions to carry electricity may be boosted by heavy precipitation of salt.

3. RESULT AND DISCUSSION

The first location of the survey line is located at the respective coordinate, as shown in Table 2. The survey is located near the major lineament in the study area. The type of array configuration used is Gradient with point A's azimuth 100° (EES) direction and point B at azimuth of 280° (WWN) direction. Figure 4 shows the setup of the equipment for survey line 1.

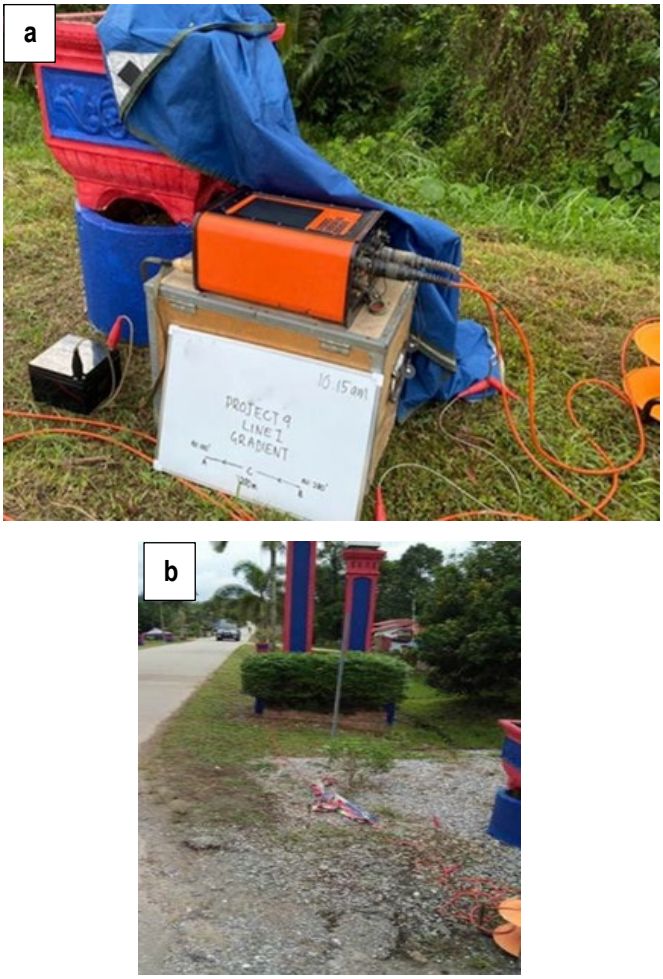

Figure 4: a) Set up for Survey Line 1 center and b) Set up for Survey Line 1 (A)

Based on Figure 5, the total RMS error for resistivity is 7.4%. In this survey line, the least amount of resistivity is 16.0 Ωm and the most is 2250 Ωm at a depth up to 36.9 m. Zone 1 has a high chance of having groundwater with a low resistivity value that is less than 115 Ωm in the depth of 13.4m to 36.9m and 6.76m to 17.3m from ground level. According to

the chargeability value, the groundwater potential area value ranges from 9 mv/v to 15 mv/v. The IP pseudosection in Figure 5 indicates that the region is sandstone, which has good porosity and permeability. For Zone 2, the chargeability value of 13mv/v to 15mv/v resistivity values range from 200 Ωm to 1500 Ωm, which is the average resistivity value for sedimentary rocks like limestone, sandstone, and shale. Zone 3 is for materials that have a high resistivity value between 1500 Ωm and 4000 Ωm, where hard materials like granite and quartzite are found. Since the study area is abundant with marble rock, Zone 3 is classified as a marble rock region, while Zone 2 is known as a limestone area because limestone undergoes the metamorphism process and forms marble rock. There are possibly five normal faults or fracture lines in this survey line, with lengths ranging from 25m to 150m and depths ranging from 1m to 36m.

Table 2: Coordinates of Electrode with Elevation

Electrode	Latitude	Longitude	Elevation (m)
1 (A)	N 04° 59' 07.6	E 102° 12' 12.2	99
21 (C)	N 04° 59' 07.4	E 102° 12' 08.9	97
41 (B)	N 04° 59' 07.0	E 102° 12' 05.7	98

The second survey line was 200 meters long, with electrode spacing of 5 meters. Respective coordinate as shown in Table 3. The array used is a Gradient configuration. The survey line is set up alongside the road. Point A was placed at 350° (NNW) and point B at 170° (ESS). Figure 6 shows the setup of the equipment for survey line 2.

Table 3: Coordinates of Electrode with Elevation

Electrode	Latitude	Longitude	Elevation (m)
1 (A)	N 04° 59' 10.6	E 102° 12' 05.1	95
21 (C)	N 04° 59' 13.8	E 102° 12' 04.7	96
41 (B)	N 04° 59' 07.2	E 102° 12' 05.6	95

Figure 7 shows that the pseudosection root-mean-square error (RMS) for resistivity is 10.3%. This survey line has a minimum resistivity of 15 m and a maximum resistivity of 1800 m at a depth of more than 37 m. The least amount of resistivity is 26.0 Ωm, and the most is 2000 Ωm at a depth up to 36.9 m. Based on the contrast of resistivity and chargeability values at 26.6Ωm to 76.7Ωm and 1mv/v to 5mv/v respectively, the potential of groundwater is identified at Zone 1 in the depth 13.4m to 36.9m. Pseudosection 2-D resistivity line 2 indicates that the topsoil at Zone 2 consists of sedimentary rock that has a resistivity value range of 100Ωm - 500Ωm, such as limestone. Since limestone has good porosity and permeability, the shallow water at a depth of 1.25m seeps through the pores and cracks into the aquifer. Zone 3 has the highest resistivity value, 600Ωm - 1880Ωm, and the highest chargeability value of 15mv/v, which shows that it consists of metamorphic or metasedimentary rock such as marble. Several possible normal faults and fracture lines are found from this survey line from the 40m to the 150m with depths from 1m to 31m.

Survey line 3 was carried out beside the Mosque of Felda Chiku 5. The array configuration used in this survey line was Pole – Dipole. Table 4 shows the coordinates and elevations of the electrodes used. Point A was located at azimuth 293° (WWN) direction, and point B at azimuth of 110° (EES) direction. Figure 8 shows the setup of the equipment for survey line 3.

Table 4: Coordinates of Electrode with Elevation

Electrode	Latitude	Longitude	Elevation (m)
1 (A)	N 04° 58' 58.7	E 102° 12' 14.5	102
21 (C)	N 04° 59' 00.2	E 102° 12' 11.6	101
41 (B)	N 04° 59' 01.0	E 102° 12' 08.4	104

This third line employs a Pole-Dipole electrode arrangement. As can be seen in Figure 9, the overall RMS error is 10%, which is more than the limit at a depth of more than 57m. The RMS error during the usage of the pole-dipole is high due to its sensitivity towards sound. This survey line has a minimum resistivity of 7.0 Ωm and a maximum resistivity of 1,600 Ωm. This result's pseudosection has three distinct regions: Zone 1, Zone 2, and Zone 3. The resistivity in Zone 1 varies from 7 Ωm to 30 Ωm. Its potential groundwater is high because a significant amount of groundwater may be stored under the surface here between 21.5 and 43.1 meters. The survey line that went right next to the river may be the reason, since it acts as a recharge agent for the groundwater. The range of the Zone 2 resistivity value is 40 Ωm to 430 Ωm. For this range of resistivity values, Zone 2 may contain sedimentary rocks such as sandstone and limestone. Because of its 1–13 mv/v chargeability rating, it has been shown to be limestone. In Zone 3, which is designated for hard materials with high resistivity values, the survey line's maximum resistivity value is 1630 Ωm. Zone 3, with the highest resistivity rating, may consist of quartzite, granite, and basalt. There are possibly three thrust faults or fracture lines in this survey line from 100m to 190m with depths of about 1m to 57m. Because the fault angle on this pseudosection is less than 45° or low angle, it can be concluded that this type of fault is a thrust fault.

Zone 1 has depths ranging from 6.8-17.3 m to 13.4-36.9 m with resistivity < 115 Ωm down to 16 Ωm. This encourages groundwater presence, especially if these strata are saturated. Groundwater exploration studies utilizing resistivity + IP often identify zones with resistivity in the 10-100 Ωm range (or slightly above) as promising for fresh groundwater in sedimentary or fractured systems (Madun et al., 2018). Matching low resistivity with moderate-to-low

chargeability (or suitable chargeability values) increases confidence; many studies combine resistivity and chargeability to eliminate ambiguity (e.g., differentiate clay/silt, saturated sand, fracture zones). In a metamorphic or basement environment, a location may have marble or severely metamorphosed rock, cracks / weathered zones wet with groundwater, which can significantly reduce resistivity, making them noticeable. Zone 2 (resistivity 200-1500 Ω·m, chargeability 13-15 mv/v) is associated with sedimentary rocks, including limestone, sandstone, and shale. Consolidated sedimentary rocks, particularly those that are dry or weakly saturated, often have resistivity values in the hundreds to thousands of Ωm. Zone 3 (resistivity 1500-4000 Ωm) includes hard materials such as granite and quartzite, as well as metamorphic rocks like marble. This is likewise similar to igneous, and many metamorphic/metasedimentary basement rocks have high resistivity when relatively fresh and unfractured (Abdelrahman et al, 2023).

Zone 1 (resistivity 26-76.7 Ω·m, chargeability 1-5 mV/V, depth 13-37 m), as possible groundwater aligns with these methods. The resistivity range is low-to-moderate, as found in previous groundwater-resistivity/IP research (Omar, 2023). A high resistivity (600-1880 Ωm) zone with high chargeability may indicate unfractured massive metamorphic/metasedimentary (e.g., marble) bedrock, where groundwater is unlikely. This is consistent with the general principle that more resistive and less conductive rock tends to be drier and less conductive to water (Abdelrahman et al, 2023). Shallow alluvium or sedimentary cover (100-500 Ω·m) with moderate resistivity may allow surface water to seep into deeper aquifers, especially if the rock is porous or fractured. This interpretation is consistent with geo-electrical studies in karst/sedimentary terrains. Zone 1 groundwater potential, Zone 2 permeable sedimentary/limestone infiltration zone, Zone 3 thick bedrock) It is a valid geophysical interpretation supported by previous studies.

The classification of resistivity zones into Zone 1 (7-30 Ωm), Zone 2 (40-430 Ωm), and Zone 3 (up to 1630 Ωm) aligns with common interpretations in ERI studies. Low resistivity zones are often associated with water-saturated or clay-rich sediments (potential aquifers), moderate resistivity with weathered or fractured rocks, and high resistivity with massive dry or bedrock. In that case, the low resistivity in Zone 1 suggests a potential groundwater-bearing layer, especially given the interpreted depth range (21.5–43.1 m). This is consistent with other studies where low-moderate resistivity zones were linked to aquifers in hard-rock terrain (Lee et al., 2021). Zone 2 may relate to sedimentary rocks (such as sandstone or limestone), which appears acceptable. Moderate resistivity values (tens to hundreds Ωm) are commonly recorded for saturated or weathered sedimentary rock or fractured carbonate, which may contain water but have lower conductivity than clayey or saturated sediments. Fault or fracture zones (100-190 m along the line, depth 1-57 m) are convincing, particularly when they line up with severe resistivity discontinuities or lateral resistivity differences. Indeed, geophysical investigations, including ERT, have relied on steep vertical or near-vertical resistivity gradients, as well as lateral shifts, to identify fault zones or heavily fractured rock (Pucci et al., 2016).

Methods in geophysics that do not need drilling, such as geoelectric and seismic approaches, can be utilized to assess subsurface features. This method is used when faults buried in the Earth are first recognized. Drilling procedures are evaluated when more precise information has been gathered. This is a more recent example of a buried (subsurface) small fault being traced with 2-D / 3-D resistivity tomography (ERT). The survey used a 1400-meter-long primary ERT line and cross-lines to locate minor fault traces. Susanto et al. (2024) found a high-resistivity layer (>250 Ωm) of rock (sandstone/basalt) with an evident discontinuity, indicating faulting. Small faulting may be buried approximately 520 meters from the first electrode. This finding was based on a discontinuity in resistivity values in the predicted basalt lava layer. A tiny fault is believed to be 160 meters below the ground surface. Basalt outcrops show that the high resistivity layer is composed of compact basalt lava covered with volcanic tuff.

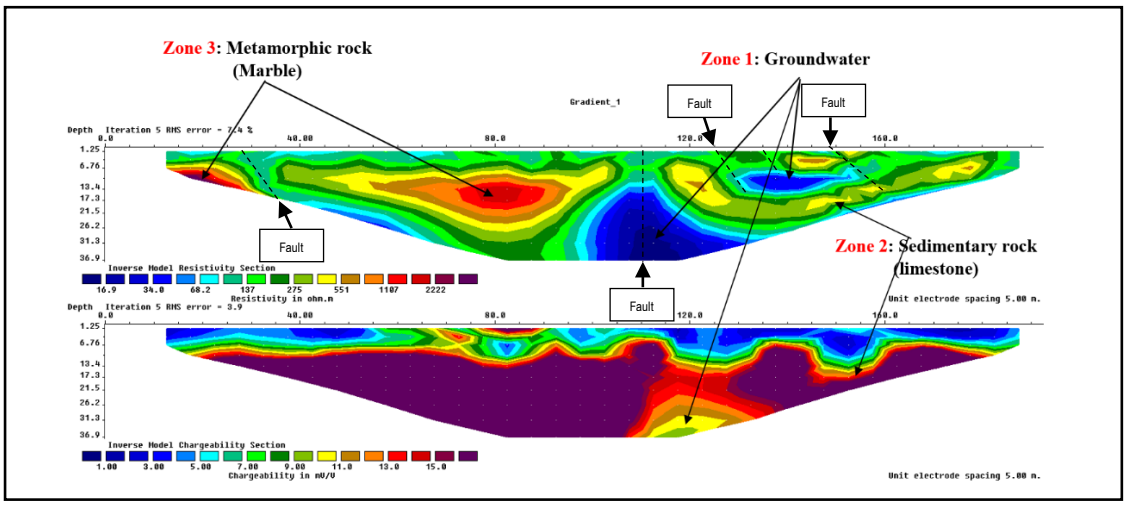

Figure 5: Survey Line 1 Pseudosection

Figure 6: Set up for Line 2

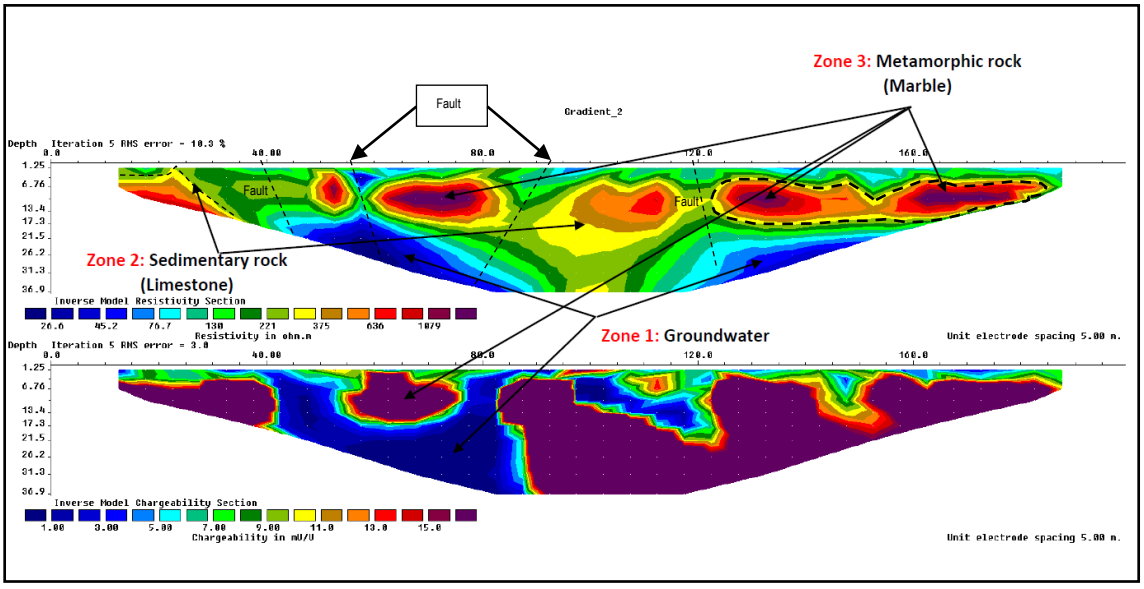

Figure 7: Survey Line 2 Pseudosection

Figure 8: Set up for Line 3

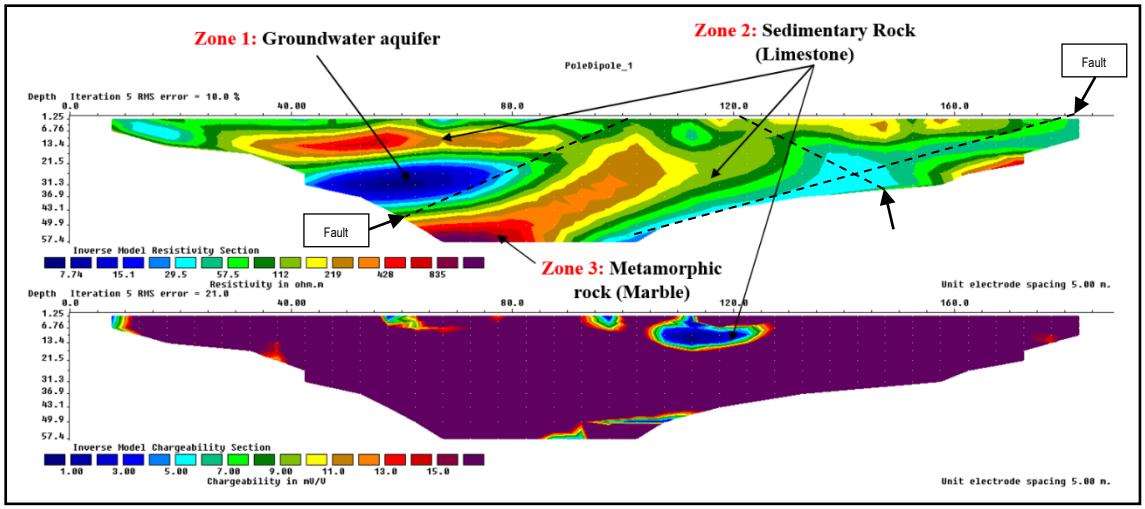

Figure 9: Survey Line 3 Pseudosection

4. CONCLUSION

This study demonstrates the use of ERI in geological structure analysis. A geological structure of potential normal faulting was revealed by the pseudosection of three survey lines, and the low-angle fracture plane (fracture line) is thought to be the result of thrust fault activity. In order to provide the amount of knowledge on subsurface geological formations for the aim of geoengineering research for site inquiry, further geophysical investigation (seismic survey) must be conducted.

According to the results of the electrical resistivity imaging study, the study's location may have shallow groundwater potential, which is consistent with the specification's topic. Combining the resistivity and chargeability measurements enhances understanding and interpretation of the underlying rock formations throughout the interpretation phase. Survey lines 1, 2, and 3 have the potential for a good groundwater aquifer at an average depth of 15 to 40 meters because of the existence of sedimentary rock limestone. It is evident from the data from three survey lines that the resistivity and conductivity values are quite similar. Earth materials with high resistance values often have lower conductivities. Since water may carry an electrical charge, conductivity evaluation has become crucial. Conversely, the resistivity indicates how water-resistant the Earth's materials are. As a result of investigations into Paloh's subsurface structures, groundwater is also helped by this effort. Future investigation should take further steps, as the project's title calls for discovering the fault zone and additional groundwater. It is necessary to do more research on the suggested drill site for borehole or core drilling to map subsurface geological features like rock type, structure, water saturation, and fracture zones. These integrated methods help validate the interpretations made from the resistivity models and ensure the accuracy of the subsurface characterization.

ACKNOWLEDGEMENT

The authors would like to express their gratitude to the Faculty of Earth Sciences, Universiti Malaysia Kelantan for their cooperation and equipment in this study.

REFERENCES

Abdelrahman, K., Hazaea, S. A., Hazaea, B. Y., Abioui, M., & Al-Awah, H. (2023). Groundwater potentiality in hard-rock terrain of southern Saudi Arabia using electrical resistivity tomography approach. *Journal of King Saud University - Science, 35*(9), Article 102928. https://doi.org/10.1016/j.jksus.2023.102928

Abidin, M. H., Madun, A., Tajudin, S. A., & Ishak, M. F. (2017). Forensic assessment on near surface landslide using electrical resistivity imaging (ERI) at Kenyir Lake area in Terengganu, Malaysia. *Procedia Engineering, 171*, 434–444. https://doi.org/10.1016/j.proeng.2017.01.354

Alamu, R., & Dada, O. J. (2025). *Structural geology: Faults, folds, and traps.*

Amadasun, C. V. O., Jegede, S. I., & Iyoha, A. (2015). Optimizing geophysical tomographic approaches in road failure of the Ozalla-Uhunmora road, near the Agor-Igbirra settlement, in Owan West Local Government Area of Edo State. *Nigerian Annals of Natural Sciences, 15*(1), 122–130.

Folk, R. L., & Bissell, H. J. (2022, April). *Sedimentary rock.* In *Encyclopedia Britannica.* https://www.britannica.com/science/sedimentary-rock

Geotomo Res2DInv. (2020). *Res2DInv.* Aarhus GeoSoftware. https://www.aarhusgeosoftware.dk/res2dinv

Hasan. (2017, October 6). *Pole-dipole array: Electrical resistivity methods, part 4.* AGIUSA. https://www.agiusa.com/pole-dipole-array-electrical-resistivity-methods

Hazreek, Z. A., Kamarudin, A. F., Rosli, S., Fauziah, A., Akmal, M. A., Aziman, M., Azhar, A. T., Ashraf, M. I., Shaylinda, M. Z., Rais, Y., Ishak, M. F., & Alel, M. N. (2018). Integral analysis of seismic refraction and ambient vibration survey for subsurface profile evaluation. *Journal of Physics: Conference Series, 995*, Article 012073. https://doi.org/10.1088/1742-6596/995/1/012073

Hussin, F., & Abdullah, H. (2012). The role of FELDA and KESEDAR in the development of land in the district of Gua Musang: A comparison the socio-economic level of the settlers. Sustainable Agriculture Research, 1(2), 284. https://doi.org/10.5539/sar.v1n2p284

Hutchison, C. T., & Denis, N. K. (2009). Geology of Peninsular Malaysia. University of Malaya and the Geological Society of Malaysia.

Kasim, S. A., Ismail, M. S., & Salim, A. M. (2020). Cenozoic stratigraphy, sedimentation and tectonic setting, onshore Peninsular Malaysia: A review. In Proceedings of the Third International Conference on Separation Technology 2020 (ICoST 2020). https://doi.org/10.2991/aer.k.201229.035

Kasim, S. A., Ismail, M. S., & Ahmed, N. (2023). Grain size statistics and morphometric analysis of Kluang-Niyor, Layang-Layang, and Kampung Durian Chondong tertiary sediments, onshore Peninsular Malaysia: Implications for paleoenvironment and depositional processes. ScienceDirect. https://www.sciencedirect.com/science/article/pii/S1018364722006620

Lee, S. C., Noh, K. A., & Zakariah, M. N. (2021). High-resolution electrical resistivity tomography and seismic refraction for groundwater exploration in fracture hard rocks: A case study in Kanthan, Perak, Malaysia. Journal of Asian Earth Sciences, 218, Article 104880. https://doi.org/10.1016/j.jseaes.2021.104880

Loke, M. H. (2001, January). Tutorial: 2-D and 3-D electrical imaging surveys. ResearchGate. https://www.researchgate.net/publication/264739285_Tutorial_2-D_and_3-D_Electrical_Imaging_Surveys

Jasin, B. (2013). Chert blocks in Bentong-Raub suture zone: A heritage of Palaeo-Tethys.

Madun, A., Tajudin, S. A. A., Sahdan, M. Z., Dan@Azlan, M. F. M., & Talib, M. K. A. (2018, December 29). Electrical resistivity and induced polarization techniques for groundwater exploration. International Journal of Integrated Engineering. https://publisher.uthm.edu.my/ojs/index.php/ijie/article/view/2668

Mah, C. H. (2018). General geology and rock slope stability analysis in Kampung Paloh 1&2, Gua Musang. UMK Eprints. http://umkeprints.umk.edu.my/9936/

Meetings of the Society. (2017). Structural geology of Gua Musang formation in Kelantan. Newsletter of the Geological Society of Malaysia. https://archives.datapages.com/data/geological-society-of-malaysia/warta-geologi-newsletter/036/036002/97a.pdf

Metcalfe, I. (2002). Permian tectonic framework and palaeogeography of SE Asia. Journal of Asian Earth Sciences, 20(6), 551–566. https://doi.org/10.1016/s1367-9120(02)00022-6

Mohamed, K. R., Mohamed Joeharry, N. A., Leman, M. S., & Ali, C. A. (2016). The Gua Musang group: A newly proposed stratigraphic unit for the Permo-Triassic sequence of northern central belt, Peninsular Malaysia. Bulletin of the Geological Society of Malaysia, 62, 131–142. https://doi.org/10.7186/bgsm62201614

Muzamil, M., Hashim, M., Abdul, M., Yusof, W., Samuding, K., Harun, N., &Baharudin, D. (2016). Application of electrical resistivity imaging technique and colloidal borescope on groundwater study at block 33, Malaysia Nuclear Agency. https://inis.iaea.org/collection/NCLCollectionStore/_Public/46/091/46091335.pdf

Omar, J. H. (2023). Geophysical investigation of groundwater resources using electrical resistivity and induced polarization method. International Journal of GEOMATE, 25(107). https://doi.org/10.21660/2023.107.s8510

Pucci, S., Civico, R., Villani, F., Ricci, T., Delcher, E., Finizola, A., Sapia, V., De Martini, P. M., Pantosti, D., Barde-Cabusson, S., Brothelande, E., Gusset, R., Mezon, C., Orefice, S., Peltier, A., Poret, M., Torres, L., & Suski, B. (2016). Deep electrical resistivity tomography along the tectonically active Middle Aterno Valley (2009 L'Aquila earthquake area, central Italy). Geophysical Journal International, 207(2), 967–982. https://doi.org/10.1093/gji/ggw308

Sean. (2019, June 18). Gradient array: Electrical resistivity methods, part 8. AGIUSA. https://www.agiusa.com/blog/gradient-array-electrical-resistivity-methods-part-8

Sulaiman, M. S., & Abiyoga, M. (2023). Application of electrical resistivity imaging (ERI) to analyse geological structure in Paloh, Gua Musang, Kelantan. BIO Web of Conferences, 73, Article 04004. https://doi.org/10.1051/bioconf/20237304004

Sulaiman, N. (2021). Determination of potential groundwater sources using electrical resistivity imaging (ERI) in Lojing, Gua Musang. IOP Conference Series: Earth and Environmental Science. https://iopscience.iop.org/article/10.1088/1755-1315/842/1/012017/pdf

Susanto, K., Harja, A., Ma'arif, F. R., & Mukhtar, H. (2024). Geophysical investigation of buried small fault beneath Western Mount Malabar using electrical resistivity tomography in the Great Bandung Basin Rim. Indonesian Journal on Geoscience, 11(3), 409–421. https://doi.org/10.17014/ijog.11.3.409-421

Thiagarajan, S., Rail, S. N., Kumar, D., & Manglik, A. (2018). Delineation of groundwater resources using electrical resistivity tomography. Arabian Journal of Geosciences, 11, Article 212.

Xin, G. W. (2018). Geology and depositional environment of Paloh area, Gua Musang, Kelantan, Malaysia. Malaysian Academic Library Institutional Repository. https://malrep.uum.edu.my/rep/Record/my.umk.eprints.9931/Description

Yao, K., Pradhan, B., & Idrees, M. O. (2017). Identification of rocks and their quartz content in Gua Musang goldfield using advanced spaceborne thermal emission and reflection radiometer imagery. Journal of Sensors, 2017, 1–8. https://doi.org/10.1155/2017/6794095

Zaid, H. A. H., Arifin, M. H., Kayode, J. S., & Iswadi, M. B. (2023). Application of 2-D electrical resistivity imaging, and induced polarization methods for delineating gold mineralization at Felda Chiku 3, Kelantan, Malaysia. Sains Malaysiana, 52(1), 305-320.

